

Triazole-Modified Triphenylene Derivative: Self-Assembly and Sensing Applications

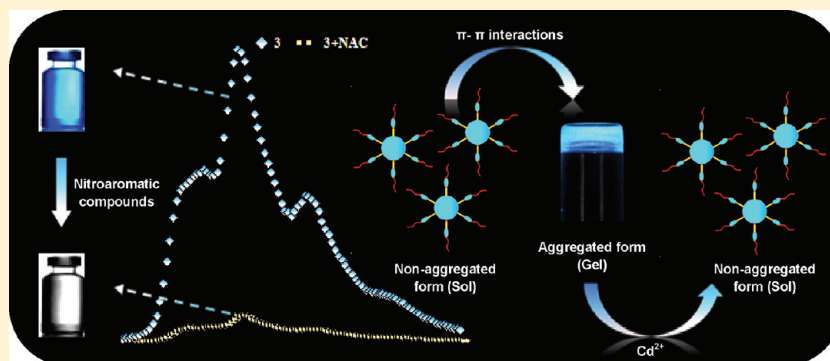
Vandana Bhalla,^{*,†} Hardev Singh,[†] Manoj Kumar,[†] and S. Krishna Prasad^{‡,§}

[†]Department of Chemistry, UGC Sponsored-Centre for Advance Studies-I, Guru Nanak Dev University, Amritsar-143005, Punjab, India

[‡]Centre for Soft Matter Research, Jalahalli, Bangalore-560013, India

 Supporting Information

ABSTRACT:



Triphenylene-based discotic liquid crystal **3** bearing 1,2,3-triazole groups has been synthesized using “click” chemistry. Discotic mesogen **3** has good thermal stability, and incorporation of triazole groups results in stabilization of columnar mesophases down to room temperature and formation of organogels in cyclohexane and mixed solvents such as hexane and dichloromethane (4:1 v/v). Characterization of the organogel of **3** in cyclohexane revealed a porous network. However, presence of Cd^{2+} ions in solution obstructed the self-assembly of this derivative due to preferred interactions between Cd^{2+} ions and triphenylene units over π – π interactions among triphenylene groups. Further, strong emission of derivative **3** in its nonaggregated form makes it a promising fluorescence sensory material for nitroaromatic compounds.

INTRODUCTION

Supramolecular assembly of molecules to form soft materials is currently a topic of great interest in areas that range from chemistry and biology to material science.^{1–3} Among various soft materials, self-assembly of discotic liquid crystals has attracted great attention because it enables formation of π -stacked columnar superstructure, which is very useful in organic electronic and optoelectronic devices,^{4–7} like organic light-emitting diodes, organic field-effect transistors, organic photovoltaic cells, gas sensors, high-resolution laser printers, and photocopying machines. Among discotics, the triphenylene (TP) derivatives have been widely studied for their liquid crystalline behavior,^{8–11} and most of them show columnar mesophase at high temperature. Although triphenylene derivatives have been widely studied in the literature, there are a few triphenylene derivatives reported to exhibit aggregation in bulk and in solution phases.^{12,13} Herein, we report the synthesis of triazole-modified triphenylene derivative **3**, which forms supramolecular aggregates both in bulk and in solution phases. The columnar assembly of TP moiety is stabilized down to room temperature in the bulk phase due to dipole–dipole interactions among 1,2,3-triazole groups. Further, strong emission of derivative **3** in DMSO and the presence of

1,2,3-triazoles permits it to work as chemosensor for nitroaromatics. To the best of our knowledge, this is the first report where a triphenylene-based receptor serves as a selective chemosensor for nitroaromatics.

RESULT AND DISCUSSION

The synthesis began with the alkylation of hexahydroxytriphenylene **1** with propargyl bromide to give precursor **2**. The final discotic molecule **3** was obtained by “click” reaction of precursor **2** with hexyl azide in the presence of CuI in 58% yield (Scheme 1).

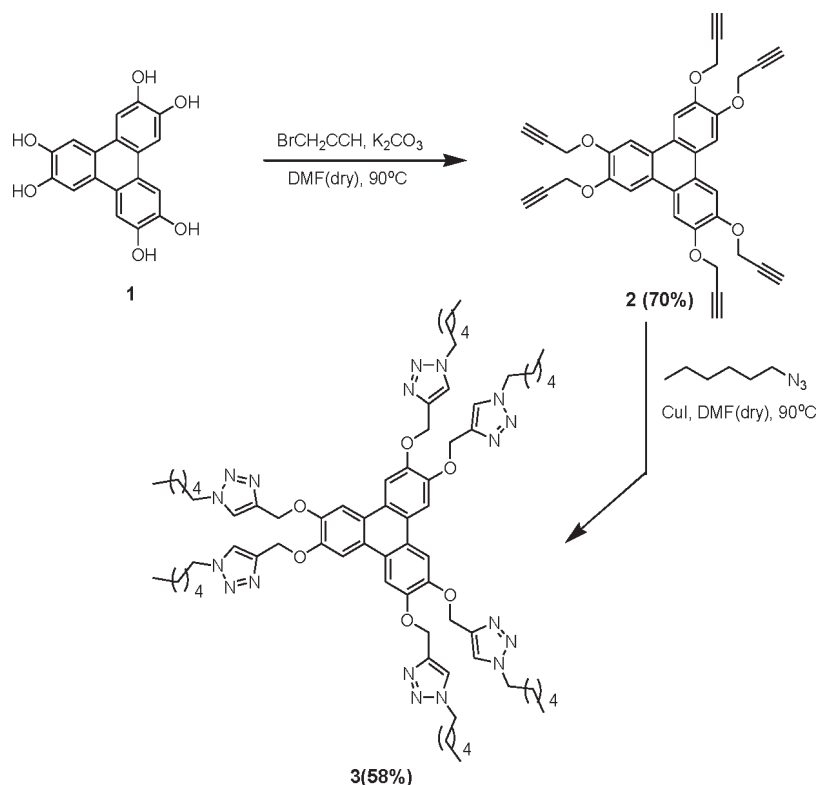
The structures of compounds **2** and **3** were characterized from their ¹H NMR, ¹³C NMR, mass, and elemental analysis (pages S13–S18, Supporting Information). ¹H NMR spectra of derivative **3** are concentration-dependent with aromatic signals moving upfield with increasing concentration (Figure S10, Supporting Information). Such an upfield shift is attributed to the intermolecular shielding from the neighboring aromatic

Received: September 27, 2011

Revised: November 9, 2011

Published: November 11, 2011

Scheme 1



molecules, suggesting their tendency to self-associate in solution through π – π interactions between neighboring molecules. Variable-temperature studies of compound 3 in CDCl₃ showed downfield shifting of aromatic protons with an increase in temperature, which suggests weakening of the aromatic π – π interactions on raising the temperature (Figure S11, Supporting Information).

The self-assembly behavior of discotic molecule 3 in bulk and solution was studied by thermogravimetric analysis (TGA), differential scanning calorimetry (DSC), polarized optical microscopy (POM), powder X-ray diffraction analysis (XRD), scanning electron microscopy (SEM) and transmission electron microscopy (TEM). TGA of compound 3 showed that it is thermally stable up to about 300 °C, and DSC analysis showed no detectable transition before the decomposition temperature (Figure S2, Supporting Information). Under POM, compound 3 exhibits hexagonal columnar phase (Col_h) down to room temperature (Figure 1).

Powder X-ray diffraction scans at 30 and 180 °C show a broad peak around 4.65 Å in the wide-angle region, which represents the averaged distance among the molten aliphatic chains surrounding the core, and another diffraction peak around 3.56 Å, which corresponds to the stacking periodicity within a column, indicating it is an ordered columnar phase (Figure 2). The mesophase was assigned as Col_h on the basis of the typical conic textures observed under POM on cooling and powder X-ray diffraction studies.

Compound 3 forms thermoreversible organogels in cyclohexane and mixed solvents such as hexane and dichloromethane (1:4) that were stable and remained stable for more than 2 months (Figure 3, inset).

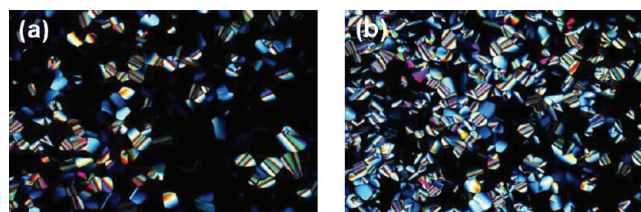


Figure 1. Polarized optical micrographs of gelator 3 at (a) 45 °C and (b) 188 °C through crossed polarizing filters.

The POM images of the organogel of compound 3 shows birefringence at room temperature, thus indicating ordered morphology in solution phase. Thermal stability of the gel was measured by the dropping-ball method.¹⁴ T_{gel} , the required temperature for the organogel to collapse, increases with an increase in concentration of gelator, as is clear from the plot of the gel to sol melting temperature, T_{gel} , against the concentration of compound 3 (Figure 3, Table 1).

The SEM and TEM images of compound 3 show networklike morphology. The morphology of structures varied across the grid, in some areas forming a dense spongelike structure (Figure 4a) and in some areas a loosely interwoven porous network (Figure 4b,c). On adding a few drops of methanol to the gel, the ordered morphology is lost and nanorods are observed (Figure 4d).

On the basis of results obtained from SEM and TEM measurements, we propose that intermolecular association based on π – π stacking, dipole–dipole, and van der Waals interactions result in the observed networklike structures. The presence of rodlike structures in the SEM image of organogel of the compound 3 indicate that the network may form from the outgrowth and subsequent enmeshing of

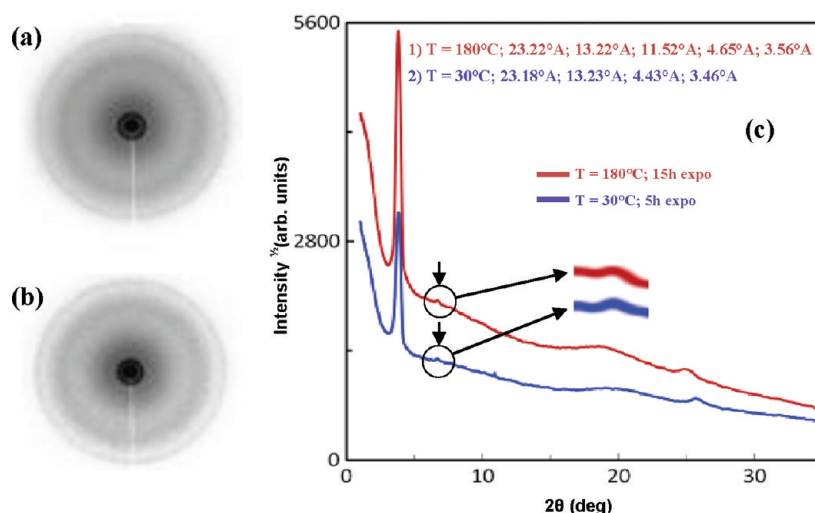


Figure 2. X-ray powder pattern of the columnar mesophase of compound 3: diffraction pattern at 30 °C (a) and 180 °C (b). (c) One-dimensional intensity profile versus 2θ .

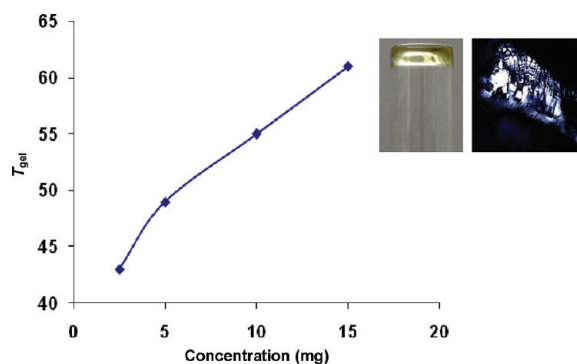
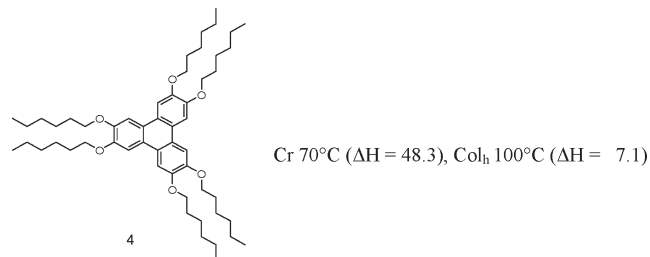


Figure 3. Variation of T_{gel} with gelator concentration of the gelator 3 in cyclohexane. The inset shows (left) organogel of gelator 3 formed in cyclohexane and (right) its polarized optical micrograph through crossed polarizing filters (magnification $\times 20$).

small rodlike structures. We also prepared compound **4**¹⁵ without 1,2,3-triazole as the control. Compound **4** is reported to exhibit liquid crystalline behavior between 70 and 100 °C. However, it displays no gelation abilities, which suggested that dipole–dipole and π – π interactions between 1,2,3-triazoles also played a synergic effect in formation of the gel. We believe that the presence of lone-pair electrons on heteroatoms in 1,2,3-triazole groups introduces a transverse dipole moment¹⁶ and triazole groups form a pseudonetwork by their dipole–dipole and π – π interactions, which stabilizes the columnar assembly of triphenylene moiety in bulk as well as in nonpolar solvents.



The UV–vis absorption spectra of compound **3** in solution and in gel phase (cyclohexane) are shown in Figure 5. The dilute

Table 1. Gelation Behavior of Compound 3

solvent used	gelation behavior ^a	amount (mg)	T_{gel} (°C) in cyclohexane
cyclohexane	G	2.5	43
	G	5.0	49
	G	10.0	55
	G	15.0	61
DCM:hexane (1:4)	G	5.0	49

^a G = gelation.

solution of compound **3** in cyclohexane displays a strong peak at 218 and a broad peak at 261 nm, corresponding to triazole and triphenylene moiety, respectively. These results indicate that π – π stacking between triphenylene and triazole moieties had an effect on the gelation process.

The self-assembling behavior of compound **3** was also examined using fluorescence spectroscopy. The most interesting observation from emission studies of compound **3** in different solvents is the decrease in fluorescence intensity with a decrease in solvent polarity (Figure 6). These studies suggest that intermolecular π – π interactions are stronger in nonpolar solvent than those in polar solvent, thus indicating greater tendency of derivative **3** to self-assemble in nonpolar solvent such as cyclohexane. The emission spectra of organogel of compound **3** in cyclohexane exhibits a significantly broadened, low intensity emission band at 471 nm (Figure S3, Supporting Information) with a bathochromic shift of 30 nm (as compared to λ_{max} 441 nm in solution).

The red-shift in the emission maxima of the gel suggests stabilization effect of aggregation in the excited state. The gel stability was tested by the influence of Cd^{2+} , Ni^{2+} , Cu^{2+} , and Hg^{2+} ions as their perchlorate salt. Interestingly, with progressive addition of 10 equiv of these cations, only gel phase treated with Cd^{2+} ions was transformed into sol phase, and in presence of Ni^{2+} , Cu^{2+} , and Hg^{2+} ions, weakening of the gel phase was observed (Figure S4, Supporting Information). We also investigated absorption and emission behavior of derivative **3** in the presence of Cd^{2+} , Ni^{2+} , Cu^{2+} , and Hg^{2+} ions as their perchlorate salt in

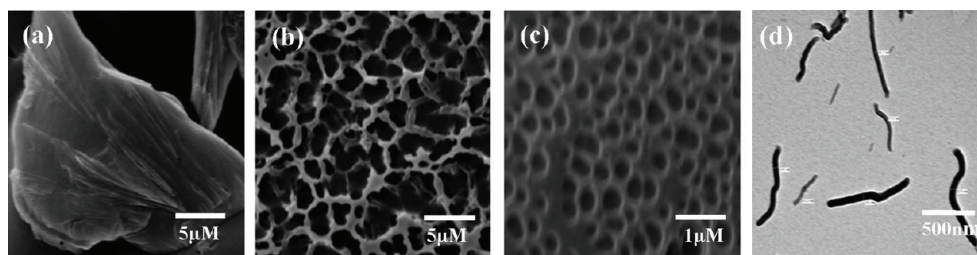


Figure 4. SEM (a–c) and TEM image (d) of the organogel of **3** formed in cyclohexane.

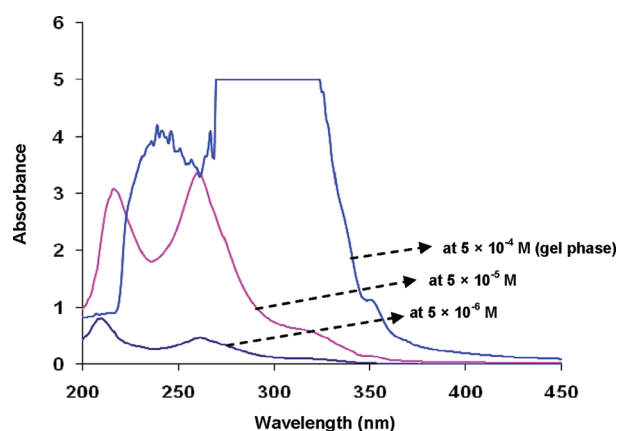


Figure 5. The UV–visible spectra of compound **3** at different concentrations in cyclohexane.

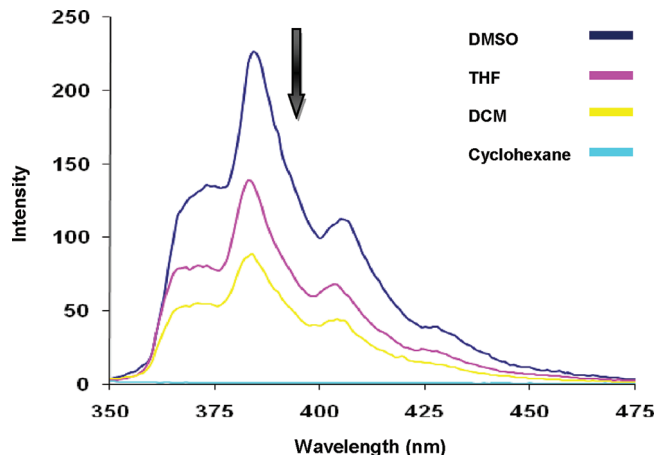


Figure 6. Fluorescence spectra of compound **3** (5×10^{-7} M), showing a decrease in emission intensity with a decrease in the polarity of solvents (slit width 3.3).

cyclohexane. Interestingly, addition of 10 equiv of cadmium ions to the solution of compound **3** (5.0×10^{-6} M) in cyclohexane leads to an enhancement of absorption intensity of bands at 218 and 261 nm, as shown in Figure 7, whereas under a similar set of conditions, addition of Ni^{2+} , Cu^{2+} , and Hg^{2+} ions led to enhancement of the absorption band at 218 nm only, and subtle changes are observed in the case of the absorption band at 261 nm. These results show that binding of compound **3** with Cd^{2+} ions destroyed the π – π stacking of both triphenylene and triazole moieties, thus leading to collapse of the gel, while in the presence of other metal ions π – π stacking between triphenylene

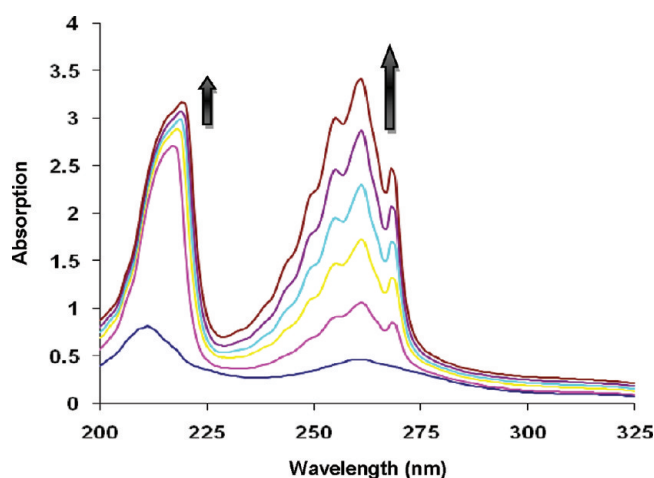


Figure 7. The UV–visible spectra of compound **3** (5.0×10^{-6} M) in the presence of Cd^{2+} (50 equiv) in cyclohexane.

units remain unaffected. These observations are corroborated by fluorescence studies, as addition of 10 equiv of cadmium ions ($15 \mu\text{L}$ THF) to the solution of compound **3** (5.0×10^{-6} M) in cyclohexane led to the appearance of a new band at λ_{max} 379 nm and the intensity of this emission band kept on increasing with further addition of 200 equiv of Cd^{2+} ions.

We assume that this phenomenon is due to a possible competition between π – π interactions among the TP units and cation– π interaction between the Cd^{2+} ions and TP units, and the latter is responsible for the blue shift of the emission band on addition of Cd^{2+} ions (Figure 8). Using the nonlinear regression analysis program SPECFIT, the binding constant ($\log \beta$) of compound **3** with Cd^{2+} was found to be 10.55. Under the same conditions as used above for Cd^{2+} ions, we also tested the fluorescence response of compound **3** to other metal ions, such as Cu^{2+} , Ni^{2+} , and Hg^{2+} , and quenching of emission was observed in the presence of these metal ions, which may be attributed to the interaction of these metal ions with triazole moieties. These observations are corroborated by ^1H NMR studies of compound **3** in the presence of Cd^{2+} ions.

Upon addition of 50 equiv of Cd^{2+} ions as their perchlorate salt to a solution of compound **3** (10 mmol) in a mixture of $\text{DMSO}-d_6$: CDCl_3 (1:4) at room temperature, we observed a substantial decrease and broadness of signal due to TP protons, suggesting interaction of Cd^{2+} ions with TP and triazole moieties, respectively (Figure S9, Supporting Information). The decrease and broadness of signal due to TP protons indicates the cation– π interactions between Cd^{2+} ions and TP unit. A similar type of Cd^{2+} – π interaction is reported in the literature.^{17,18}

Hexasubstituted triphenylenes are attractive building blocks, combining synthetic and structural advantages, low cost materials, the possibility of substitution at the periphery, potential π -interactions, as well as photophysical properties. However, numerous possibilities exist for the use of triphenylene derivatives in host–guest chemistry, in general. There are few reports in the literature that exploit the metal complexation behavior of triphenylene.¹⁹ Recently, there has been a lot of activity in the design and synthesis of quick and reliable chemosensors for detection of nitroaromatic compounds in an effort to better combat terrorism and control pollution.^{20–22} Nitroaromatic compounds (NAC) such as dinitrotoluene (DNT), dinitrobenzene (DNB), and picric acid (PA) are well-known primary constituents of many unexploded land mines worldwide and

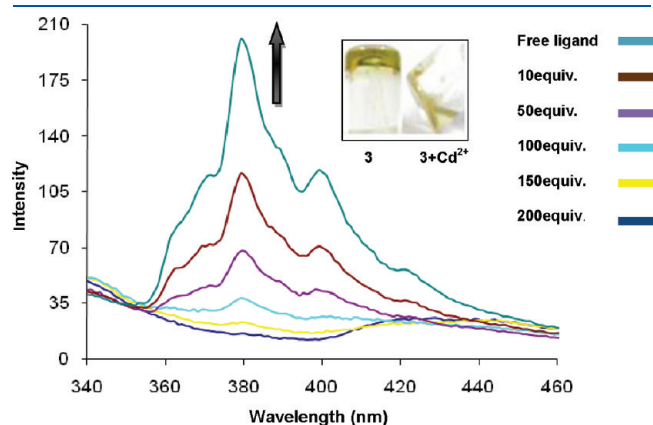


Figure 8. The fluorescence spectrum of **3** (5×10^{-6} M) in the presence Cd^{2+} ions (up to 200 equiv) in cyclohexane. The inset shows the destruction of the self-assembly of **3** in the presence of Cd^{2+} ions.

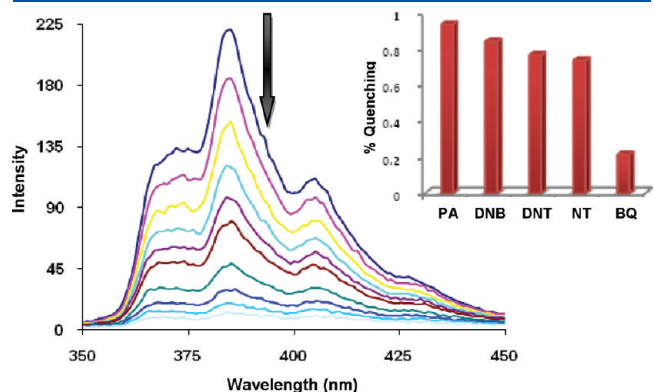


Figure 9. Fluorescence quenching of **3** (5×10^{-7} M) upon the incremental addition of picric acid (270 equiv) in DMSO.

are also considered environmental contaminants and toxic to living organisms,^{23–26} as the soil and groundwater of the war zone and military facilities can contain toxic levels of these compounds and their degradation products. For sensing of nitroaromatic compounds, π -electron rich aromatic compounds are desirable, as is evident from the literature reports.²⁷ We envisaged that polyaromatic electron-rich derivative **3** must be an ideal candidate for sensing nitroaromatics. Thus, we studied the binding behavior of compound **3** toward different NAC such as DNT, DNB, PA, nitrotoluene (NT), and benzoquinones (BQ). We employed DMSO as solvent in all the fluorescence studies, as derivative **3** exists in unassembled form in DMSO and its solution in DMSO shows a quantum yield of $\Phi = 0.31$. The fluorescence spectrum of **3** (5.0×10^{-7} M) in DMSO exhibits an emission band at λ_{max} 383 nm with two shoulders at 371 and 403 nm when excited at 278 nm). Upon addition of picric acid (270 equiv), the fluorescence emission is completely quenched (Figure 9).

The quenching of compound **3** was observed with of DNT acid (520 equiv), DNB (500 equiv), NT (650 equiv), and BQ (5000 equiv) (Figures S6 and S7, Supporting Information). The results of fluorescence studies of compound **3** in DMSO with DNT, DNB, NT, and BQ are summarized in Figure 9 (inset), and it is evident that the most electron-deficient aromatic substrates engendered the greatest quenching; i.e., the greater the number of electron-withdrawing nitro (NO_2) groups present on the benzene/toluene core, the more extensive the degree of fluorescence quenching. This finding is consistent with the proposed mechanism, in which nitroaromatic analyte acts as fluorescence quencher as the result of a charge-transfer event. For solid-state detection of nitroaromatics, we exposed organogel of derivative **3** in cyclohexane to vapors of picric acid by inserting the vial containing organogel into a sealed vial at room temperature containing solid picric acid and cotton gauze, which prevents direct gel–analyte contact and helps to maintain a constant vapor pressure. The complete gel to sol transition was observed in 8 h (Figure 10). The SEM image of sol shows an absence of

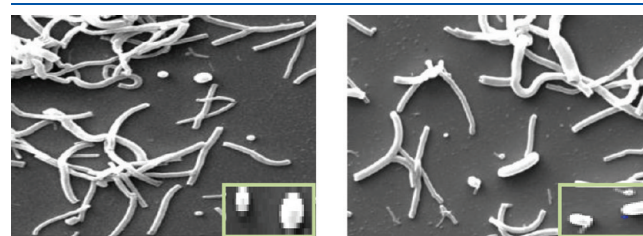


Figure 11. SEM images of organogel of gelator **3** after the vapor diffusion of picric acid in cyclohexane. The inset show the picric acid nanospheres.

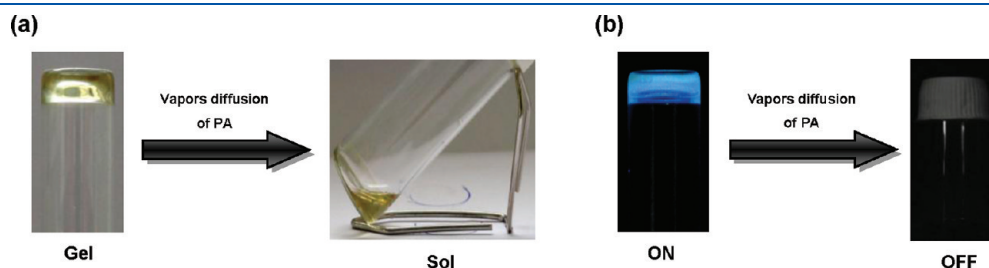


Figure 10. (a) gel to sol transition and (b) fluorescence quenching of gelator **3** by the vapor diffusion of picric acid in cyclohexane.

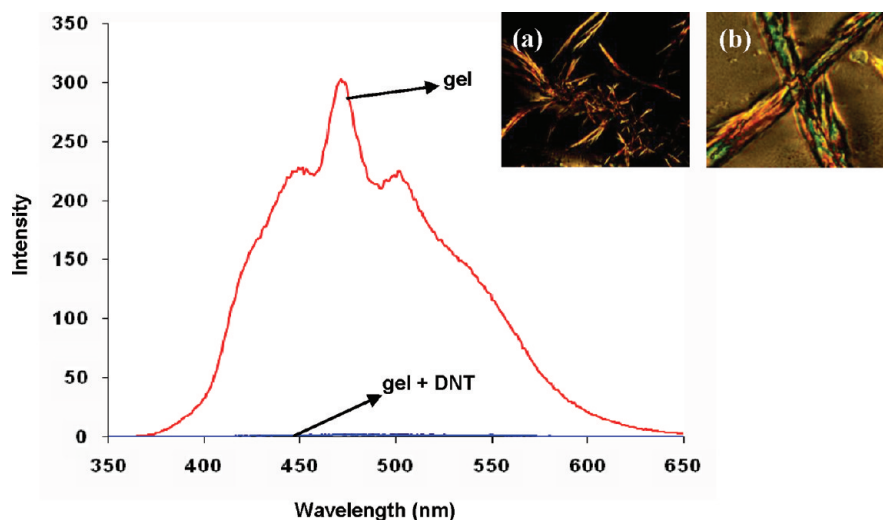


Figure 12. Fluorescence spectra of the gel of compound **3** in the presence of 3.5 equiv of DNT in cyclohexane. The inset shows the POM images of the gel of **3** formed by mixing the different equivalents of DNT, (a) 1.5 equiv and (b) 3.5 equiv, through crossed polarizing filters.

networklike structure due to obstruction of the supramolecular assembly in the presence of picric acid (Figure 11).

The good solubility of DNT in cyclohexane prompted us to investigate organogel formation of **3** in cyclohexane in the presence of DNT. Interestingly, gelation of derivative **3** in cyclohexane was observed in the presence of 1.5, 2.5, and 3.5 equiv of DNT (w/w), and the POM images of the organogels of compounds **3** with different amounts of DNT show birefringence at room temperature (Figure 12). However, a further increase in the amount of DNT leads to appearance of solid particles in the gel. The fluorescence study of the organogel of compound **3** in cyclohexane in the presence of 3.5 equiv of DNT shows quenched emission.

EXPERIMENTAL SECTION

General Information. All chemicals and reagents were purchased from Sigma Aldrich and were used as such without further purification. The solvents were obtained from the commercial sources and used as such, except THF, which was dried over the sodium prior to use. Silica gel 60 (60–120 mesh) was used for column chromatography. The fluorescence spectra were recorded on a Shimadzu RF 5301 PC spectrofluorometer. The UV–vis spectra were recorded on a Shimadzu UV-2450 spectrophotometer. All NMR spectra were recorded on a JEOL-FT NMR-AL 300 MHz spectrophotometer using CDCl_3 and $\text{DMSO}-d_6$ as solvents and TMS as internal standard. Data are reported as chemical shifts in ppm (δ), multiplicity (s = singlet, d = doublet, br = broad singlet, m = multiplet), coupling constants (Hz), integration, and interpretation. MALDI-TOF spectra were recorded on a Bruker Daltonics flexAnalysis instrument. FAB mass spectra were recorded on a JEOL SX 102/Da-600 mass spectrometer. Elemental analysis (C, H, N) was performed on a Flash EA 1112 CHNS-O analyzer (Thermo Electron Corp.). Polarized optical microscopy (POM) was recorded on a Nikon ECLIPSE LV100 POL. Thermogravimetric analysis (TGA) was recorded on an EXSTAR TG/DTA 6300 at a heating range of 10 $^\circ\text{C}/\text{min}$ under a nitrogen environment. Differential scanning calorimetry (DSC) was recorded on a Perkin-Elmer DSC7. Scanning electron microscope (SEM) measurements were recorded on a JEOL JSM-5600 LV scanning electron microscope at 10 kV.

Synthesis of 2,3,6,7,10,11-Hexakis(prop-2-ynyloxy)triphenylene (2). To a solution of hexahydroxytriphenylene (900 mg, 2.77 mmol) in dry DMF (5 mL) was added K_2CO_3 (3.45 g, 25 mmol),

and mixture was stirred at room temperature for 10–15 min. Then propargyl bromide (2.97 g, 25 mmol) was added dropwise and slowly with continued stirring of the reaction mixture. The resulting mixture was heated at 60–70 $^\circ\text{C}$ overnight. After the completion of the reaction, excess water was added. The solid was separated out, which was filtered off and washed with water to get the crude product. The crude product was recrystallized from DCM and methanol to get the titled compound as yellow solid in 70% yield. ^1H NMR (300 MHz, $\text{DMSO}-d_6$, δ ppm): 3.62 (s, 6 H), 5.09 (s, 12 H), 8.13 (s, 6 H). ^{13}C NMR (75.45 MHz, $\text{DMSO}-d_6$, δ ppm): 56.51, 78.68, 79.06, 107.82, 123.21, 146.83. (FAB+) MS m/z : 576 ($\text{M} + \text{Na}$) $^+$. Anal. Calcd for $\text{C}_{36}\text{H}_{24}\text{O}_6$: C, 78.25; H, 4.38. Found: C, 77.98; H, 4.18.

Synthesis of 4-((2,3,6,7,10-Pentakis((1-hexyl-1H-1,2,3-triazol-4-yl)methoxy)triphenylene-11-yloxy)methyl)-1-hexyl-1H-1,2,3-triazole (3). A solution of **2** (706 mg, 1.27 mmol), hexyl azide (1.17 g, 9.2 mmol), and Cu^{I} was heated in dry DMF (5–6 mL) at 90 $^\circ\text{C}$ overnight. The mixture was then diluted with DCM and washed with water and then brine. The organic layer was separated and dried over Na_2SO_4 , and the solvent was evaporated under reduced pressure to get the crude product, which was purified by column chromatography to give the pure compound **3** as a yellowish-brown solid in 58% yield. ^1H NMR (300 MHz, CDCl_3 , δ ppm): 0.82 (t, $J = 6.9$ Hz, 18 H), 1.25 (br, 36 H), 1.87 (s, 12 H), 4.33 (t, $J = 7.2$ Hz, 12 H), 5.55 (s, 12 H), 7.88 (s, 6 H), 8.06 (s, 6 H). ^{13}C NMR (75.45 MHz, CDCl_3 , δ ppm): 13.85, 22.32, 26.12, 30.17, 31.07, 50.35, 63.23, 108.07, 123.50, 123.69, 143.88, 147.81. MALDI-TOF MS m/z : 1317 ($\text{M} + 2$) $^+$. Anal. Calcd for $\text{C}_{72}\text{H}_{101}\text{N}_{18}\text{O}_6$: C, 65.78; H, 7.74; N, 19.18. Found: C, 65.53; H, 7.43; N, 18.88.

CONCLUSION

In conclusion, we have synthesized triphenylene derivative **3**, which forms supramolecular aggregates in bulk as well as in solution phases, using “click” chemistry. The gel-to-sol phase transition process can be selectively controlled by interaction with Cd^{2+} ions. Interestingly, electron rich derivative **3** works as an efficient and sensitive fluorescent sensor for nitroaromatic explosives.

ASSOCIATED CONTENT

S Supporting Information. $^1\text{H}/^{13}\text{C}$ NMR, FAB mass, concentration- and temperature-dependent NMR studies, fluorescence spectra with different metal ions and nitro derivatives,

DSC, and TGA studies. This information is available free of charge via the Internet at <http://pubs.acs.org>.

AUTHOR INFORMATION

Corresponding Author

*E-mail: vanmanan@yahoo.co.in.

Notes

[§]Responsible for powder X-ray diffraction studies.

ACKNOWLEDGMENT

V.B. is thankful to DST (New Delhi, India) (ref no. SR/S1/OC-63/2010) and DRDO (ref no. ERIP/ER/0703663/M/01/1105) for financial support. We are also thankful to National Institute for Interdisciplinary Science and Technology (NIIST) Thiruvananthapuram, Kerala, India, for SEM and TEM studies.

REFERENCES

- (1) Lehn, J. M. *Supramolecular Chemistry: Concepts and Perspectives*; Wiley-VCH: Weinheim, Germany, 1995.
- (2) James, D. K.; Tour, J. M. In *Nanoscale Assembly Techniques*; Huck, W. T. S., Ed.; Springer: New York, 2005.
- (3) Hirst, A. R.; Escuder, B.; Miravet, J. F.; Smith, D. K. *Angew Chem., Int. Ed.* **2008**, *47*, 8002.
- (4) Schmidt-Mende, L.; Watson, M.; Müllen, K.; Friend, R. H. *Mol. Cryst. Liq. Cryst.* **2003**, *396*, 73.
- (5) Hassheider, T.; Benning, S. A.; Lauhof, M. W.; Kitzerow, H. S.; Bock, H.; Watson, M. D.; Müllen, K. *Mol. Cryst. Liq. Cryst.* **2004**, *413*, 461.
- (6) Oukachmih, M.; Destruel, P.; Seguy, I.; Ablart, G.; Jolinat, P.; Archambeau, S.; Mabiala, M.; Fouet, S.; Bock, H. *Sol. Energy Mater. Sol. Cells* **2005**, *85*, 535.
- (7) Bayer, A.; Zimmermann, S.; Wendorff, J. H. *Mol. Cryst. Liq. Cryst.* **2003**, *396*, 1.
- (8) Kumar, S. *Liquid Cryst.* **2004**, *31*, 1037.
- (9) Pal, S. K.; Kumar, S. *Liquid Cryst.* **2008**, *35*, 381.
- (10) Kohmoto, S.; Mori, E.; Kishikawa, K. *J. Am. Chem. Soc.* **2007**, *129*, 13364.
- (11) Manickam, M.; Belloni, M.; Kumar, S.; Varshney, S. K.; Rao, D. S. S.; Ashton, P. R.; Preece, J. A.; Spencera, N. *J. Mater. Chem.* **2001**, *11*, 2790.
- (12) Zhao, B.; Liu, B.; Png, R. Q.; Zhang, K.; Lim, K. A.; Luo, J.; Shao, J.; Ho, P. K. H.; Chi, C.; Wu, J. *Chem. Mater.* **2010**, *22*, 435.
- (13) Kotlewski, A.; Norden, B.; Jager, W. F.; Picken, S. J.; Mendes, E. *Soft Matter* **2009**, *5*, 4905.
- (14) Debnath, S.; Shome, A.; Dutta, S.; Das, P. K. *Chem. Eur. J.* **2008**, *14*, 6870.
- (15) Boden, N.; Bushby, R. J.; Liu, Q.; Lozman, O. R. *J. Mater. Chem.* **2001**, *11*, 1612.
- (16) Lai, L. L.; Wang, C. H.; Hsieh, W. P.; Lin, H. C. *Mol. Cryst. Liq. Cryst.* **1996**, *287*, 177.
- (17) Huston, M. E.; Engleman, C.; Czarnik, A. W. *J. Am. Chem. Soc.* **1990**, *112*, 7054.
- (18) Choi, M.; Kim, M.; Lee, K. D.; Han, K. N.; Yoon, I. A.; Chung, H. J.; Yoon, J. *Org. Lett.* **2001**, *3*, 3455.
- (19) Chen, L.; Kim, J.; Ishizuka, T.; Honsho, Y.; Saeki, A.; Seki, S.; Ihee, H.; Jiang, D. *J. Am. Chem. Soc.* **2009**, *131*, 7287.
- (20) Yinon, J. *Anal. Chem.* **2003**, *75*, 99A.
- (21) Rouhi, A. M. *Chem. Eng. News* **1997**, *75*, 14.
- (22) Steinfeld, J. I.; Wormhoudt, J. *Annu. Rev. Phys. Chem.* **1998**, *49*, 203.
- (23) Ownby, D.; Belden, J.; Lotufo, G.; Lydy, M. *Chemosphere* **2005**, *58*, 1153.
- (24) Etnier, E. L. *Regul. Toxicol. Pharmacol.* **1989**, *9*, 147.

(25) Honeycutt, M. E.; Jarvis, A. S.; McFairland, V. A. *Ecotoxicol. Environ. Saf.* **1996**, *35*, 282.

(26) Lachance, B.; Robidoux, P. Y.; Hawari, J.; Ampleman, G.; Thiboutot, S.; Sunahara, G. I. *Mutat. Res., Genet. Toxicol. Environ. Mutagen.* **1999**, *444*, 25.

(27) Shanmugaraju, S.; Joshi, S. A.; Mukherjee, P. S. *J. Mater. Chem.* **2011**, *21*, 9130.